Available online at www.sciencedirect.com
ScienceDirect
Journal of Power Sources 159 (2006) 491–500
JOURNAL OF POWER SOURCES
www.elsevier.com/locate/jpowsour

Analysis of the polarization of a direct methanol fuel cell using a pseudo-reversible hydrogen reference electrode

Yo Jin Kim [a], Won Hi Hong [a,*], Seong Ihl Woo [a], Hong Kee Lee [b]

[a] *Department of Chemical and Biomolecular Engineering, KAIST, 373-1 Kusong-dong, Yusong-gu, Taejon 305-701, Republic of Korea*
[b] *Korea Institute of Industrial Technology, 472 Kajwa 4-dong, Seo-Ku, Incheon 404-254, Republic of Korea*

Received 29 August 2005; received in revised form 29 October 2005; accepted 2 November 2005
Available online 13 December 2005

Abstract

In order to observe the performance of the anode and cathode during actual direct methanol fuel cell (DMFC) operating conditions and to minimize the polarization of the reference electrode, we used a reversible hydrogen reference electrode (RHE) with its instability minimized. For analysis of the *I–V* polarization curve of each electrode, Tafel plots were used as the diagnostic tool. According to the slopes in the Tafel plot, the *I–V* polarization curves of each electrode were divided into the several regions. The effects of operating parameters on the performance of each electrode were interpreted in terms of mass transfer and electrode activation. The methanol and oxygen crossover through the membrane significantly affected the performance of the cell.

Keywords: Direct methanol fuel cell; Hydrogen reference electrode; Tafel plot; Methanol crossover; Voltammetry; *I–V* polarization

1. Introduction

The direct methanol fuel cell (DMFC) is very attractive for small and portable energy systems. Methanol is a convenient liquid fuel at room temperature, has limited toxicity, is inexpensive, and has a high energy density. Compared to other fuel cell systems, the DMFC has the advantages of a low temperature of operation, easy fuel storage and transport and a simple design that does not require a reformer.

The effects of the operating conditions on the performance of DMFCs have been studied by many researchers. DMFCs can be operated using either a vapor methanol feed or a liquid methanol feed. The latter type has been preferred because of its lower thermal requirements in spite of its poor mass transfer characteristics and high methanol crossover [1,2]. During the operation of a liquid-feed DMFC, operating parameters such as temperature, concentration, and reactant flow rate should be optimized. For example, too low a concentration of methanol causes a high concentration polarization and too high a concentration of methanol leads to high methanol membrane-permeation rates. Similarly, temperatures that are too high cause a dramatic increase in methanol cross-over rates leading to low fuel utilization and lower cell voltage while the performance of the DMFCs at high temperatures can be improved by taking advantage of the pronounced thermal activation of the electrochemical reactions.

Methanol crossover is a critical obstacle for the enhancement of DMFC performance as it causes performance losses at the cathode and lost fuel. In earlier studies, several researchers measured the methanol permeation rate by equilibrating the polymer electrolyte with a methanol or methanol/electrolyte solution [3–6]. During cell operation, methanol crossover has usually estimated by measuring cathodic CO_2 flux under the assumption that CO_2 flux from the cathode of a DMFC is wholly attributed to methanol crossover [7–14]. However, CO_2 diffuses through Nafion at up to 1×10^{-8} mol cm^{-1} s^{-1} at room temperature, and therefore, CO_2 permeation may not be negligible. Recently, CO_2 that had permeated from the anode was corrected by measuring the permeation rate of CO_2 through the membrane [12–14]. Also recently, an electrical method using the DMFC single cell directly was developed [15,16]. In this method, N_2 was introduced on the cathode side and a positive voltage was applied using a power supply. The reaction occurring at the cathode is the oxidation of the methanol that crosses through the membrane. When the applied voltage is high enough to quickly oxidize all

* Corresponding author. Tel.: +82 42 869 3919/3959; fax: +82 42 869 3910.
E-mail address: whhong@kaist.ac.kr (W.H. Hong).

0378-7753/$ – see front matter © 2005 Elsevier B.V. All rights reserved.
doi:10.1016/j.jpowsour.2005.11.001

of the methanol diffusing to the cathode side, a limiting current is achieved. This limiting current represents approximately the rate of methanol crossover at the open circuit. Both the diffusion coefficient and the methanol concentration in the membrane were determined from the measured transient limiting current density following a potential step. Heinzel and Barragán [17] reviewed the state of the art of the methanol crossover. They summarized the effect of operating parameters on methanol crossover and fuel cell performance.

For diagnosing the polarization of DMFC cells, many researchers have used reference electrodes. Reference electrodes that have been used in polymer electrolyte fuel cell (PEMFC)s or DMFCs can be classified as either pseudo-DHE (dynamic hydrogen electrode) or pseudo-RHE (reversible hydrogen electrode) types. The most frequently used reference electrodes are the asymmetrical DHE in which N_2 or H_2 gas flows into the cathode, enabling the cathode to become a H_2 evolution electrode as a pseudo DHE and allowing the anode to act as a counter electrode of the cathode [8,13,18–22]. Using this reference electrode, Narayanan et al. [8] observed that the polarization at high current densities resulted from the air electrode, and that the methanol electrode was the most significant contributor to the polarization at low/medium current densities for 1 and 2 M methanol solutions. Dohle et al. [13] confirmed the enhancement of anode performance, especially in the mass-transfer dominant regime, with the increase of methanol concentration. This reference electrode does have some convenient properties with respect to ease of use. However, it showed some overpotential related to impurities such as O_2 and the original resistance of H_2 evolution electrode, which is a particularly serious at low current density [23]. Recently, Kuver et al. [24] developed an additional DHE system in which an additional pair of Pt wires or Pt-coated electrodes was put in direct contact with the membrane and a small cathodic current was constantly applied to the electrode. This system has been used by several researchers [23–26]. Ren et al. [23] checked the reliability of this reference electrode in detail and found that it could be a good candidate for a polymer electrolyte fuel cell electrode. However, at high current density, the H_2 evolution at this electrode showed a large polarization due to the decreased activity of H^+. Therefore, recently, for the diagnosis of polarizations in the DMFC, Kuver et al. [24] used an additional DHE system at low temperature and pressure and an asymmetric DHE system at high temperature and pressure. For RHE, due to its inherent sensitivity, which is related to hydrogen coverage and poisoning, careful operation is required [24]. It could be externally equipped through a liquid electrolyte salt bridge or could be put in direct contact with a polymer electrolyte. Gurau et al. [27] used this RHE to estimate the performance of various anode catalyst materials for DMFCs and Jaouen et al. [28] interpreted the polarization curve of PEMFC with RHE.

The object of this work is to diagnose the *I–V* polarization curve using a pseudo-RHE reference electrode and to interpret the effect of operating parameters and the interaction between the anode and the cathode in a single cell. In order to observe the interaction of the anode and the cathode during actual DMFC operation condition and minimize the polarization of the reference electrode, we used the RHE reference electrode with minimal instability.

2. Experimental

2.1. Preparation of the MEA and the electrode

Two types of membrane electrode assemblies (MEAs), "type A" and "type B," were prepared. The catalyst ink was identical for both MEAs. Pt black and PtRu black (from Johnson-Matthey Inc.) were used as the catalysts for the cathode and the anode, respectively. Catalyst inks were prepared by dispersing the catalysts, water, isopropyl alcohol, and 5% Nafion ionomer solution and were brushed onto carbon paper. As described below, the two types of MEAs had a different gas diffusion electrode (carbon paper + gas diffusion layer) but had the same catalyst loading.

2.1.1. Type A

Carbon paper, TGP 090 (from Toray Inc.) was wet-proofed with FEP solution and a heat-treatment. The slurry of the diffusion layer consisted of carbon (Vulcan X), PTFE and IPA. This was brushed onto the carbon paper and was also heat-treated. The catalyst loading was 5 mg cm^{-2}. Nafion 117 was used as the polymer electrolyte.

2.1.2. Type B

Commercial carbon paper, SCL carbon Sigracet® SGL20BC (from SGL carbon group Inc.) was used. The catalyst loading was 5 mg cm^{-2}. Nafion 115 was used as the polymer electrolyte.

2.2. Operation with reference electrode

A schematic diagram of a single cell is shown in Fig. 1.

A reference hydrogen electrode was equipped with the usual cell hardware and was tested as a reference electrode, following the works of Ren et al. [23] and Gurau et al [27]. The RHE electrodes were a pair of Pt-black coated carbon electrode with an

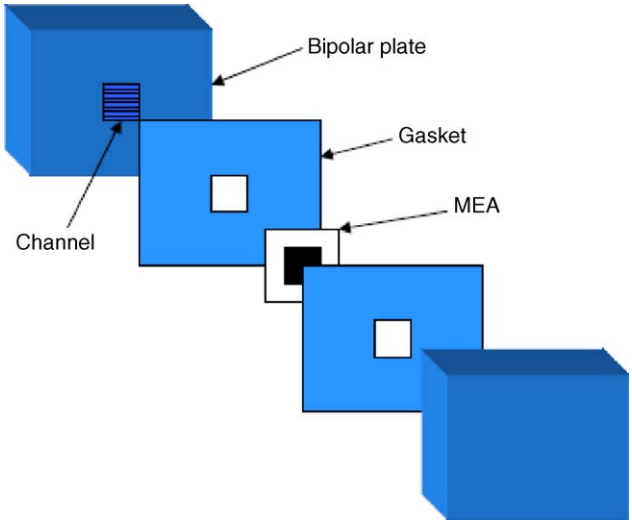

Fig. 1. Scheme of unit cell for DMFC.

area of 1 m^2 and were hot-pressed onto Nafion. The edge of the reference electrode was separated from the fuel cell electrodes edges by 3 cm in order to minimize the deactivation of the reference electrode by methanol. The reference electrode was affixed to the end of a Teflon plug that had a H_2 gas port. In H_2 flow, the reference electrode was able to obtain reversibility. Leakage of hydrogen from the RHE into the anode was prevented by means of an O-ring. During the operation of the DMFC, the methanol solution was fed to the inlet of the anode (at the bottom of the cell) and O_2 was fed into the inlet of the cathode (at the top of the cell). H_2 was fed into the additional Teflon cell on the DHE electrodes. All gas feed streams were saturated by water vapor. Since the proton activity near the RHE should be constant during each measurement, the humidification of H_2 is important. The polarization curves were IR corrected. To check the reliability of the reference electrode, we performed the following procedure for each measurement. We checked:

(i) Whether or not the OCV (open circuit voltage) of the cell had changed after flowing H_2 into the reference electrode: i.e., if H_2 had leaked into the MEA or not.
(ii) Whether or not the stabilized OCV of the cell after the loading and subsequent unloading of the current was the same as the OCV before the loading: i.e., if the electro-osmosis of methanol and water had perturbed the potential of RHE.
(iii) Whether or not the potentials between the reference electrode and the cathode or the anode, without the current loaded to the cell, remained stable potentials with continuous H_2 blowing into RHE: i.e., if, indirectly, the diffusion of methanol had degraded the performance of RHE.

All electrochemical measurements for the cell were performed after the sufficient equilibration under the open circuit. The *I–V* polarization curve was obtained by applying a step current until the potential of each electrode potential was sustained at a pseudo-steady state.

2.3. Measurement with rotating disk electrode for the observation of mixed potential behavior

The mixed potential behavior between oxygen reduction and methanol oxidation was explored with a rotating disk electrode. In order to prepare the modified thin film electrode, catalysts were dispersed ultrasonically in water at a concentration of 4 mg ml^{-1} and 20 μl of aliquot was transferred onto a polished glassy carbon substrate. After the water evaporated, the resulting thin film of the catalysts was covered with 5 wt.% Nafion solution and was used as a working electrode. A 1 M ClO_4(aq) solution was used as an electrolyte solution, after being purged with Ar for at least 30 min. Several microliters of methanol were added into the electrolyte in order to investigate the effect of methanol oxidation on oxygen reduction. In addition, in order to study the effect of oxygen reduction on methanol oxidation, we used the 2 M methanol electrolyte solution, blowing O_2 flow into the electrolyte solution with specific flow rates. The reference electrode was a Ag/AgCl electrode and the counter electrode was a long platinum wire. Potential was scanned from 1.0 V (versus NHE) to 0.5 V with a scan rate of 15 mV s^{-1}. The rotating disc electrode measurements were performed at a rotation speed of 4000 rpm. O_2 flow was fixed at 350 cm^3 min^{-1}.

3. Results

In Figs. 2 and 3, the polarizations curves of "type A" MEA and "type B" MEA were compared for the anode and cathode, respectively.

As shown in Fig. 2, for both types of MEA, the open circuit potentials of the anode were lower with higher temperatures and were not affected significantly by the concentration of methanol. Obviously, the higher temperature could activate the anode thermodynamically. In addition, at the low current region where activation polarization is dominant, the effect of temperature is more significant than the effect of the concentration of methanol. In the electro-oxidation reaction equation, the reaction rate is determined exponentially by the temperature. For DMFC operation, a large excess of water relative to methanol is applied. Therefore, the effect of methanol concentration is much smaller, compared with the effect of temperature in the activation polarization-dominant region. When the anode polarizations of both MEAs were compared, the anode polarization of "type B" MEA showed the effect of concentration from

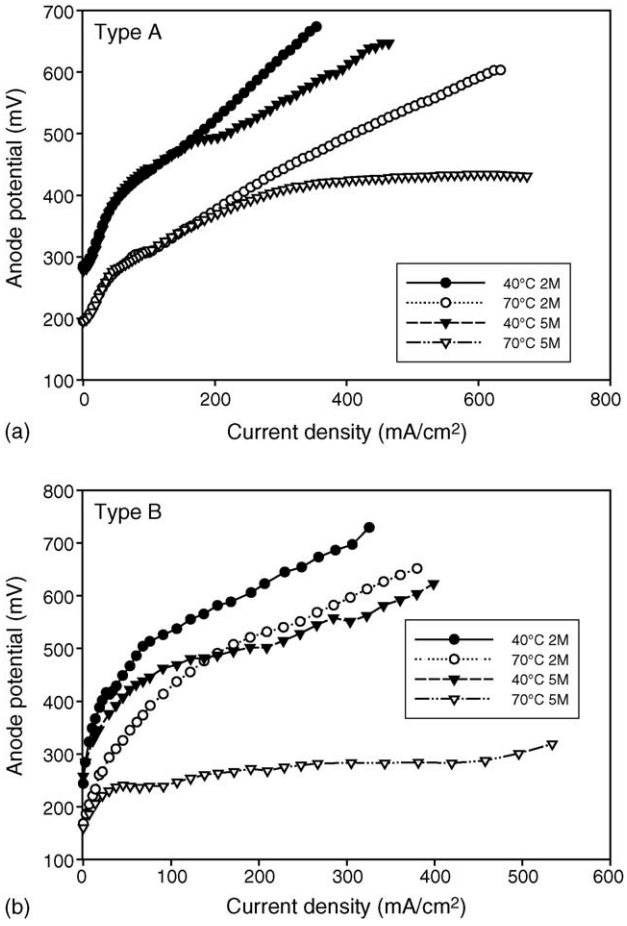

Fig. 2. Comparison of anode polarization curve (a) type A and (b) type B.

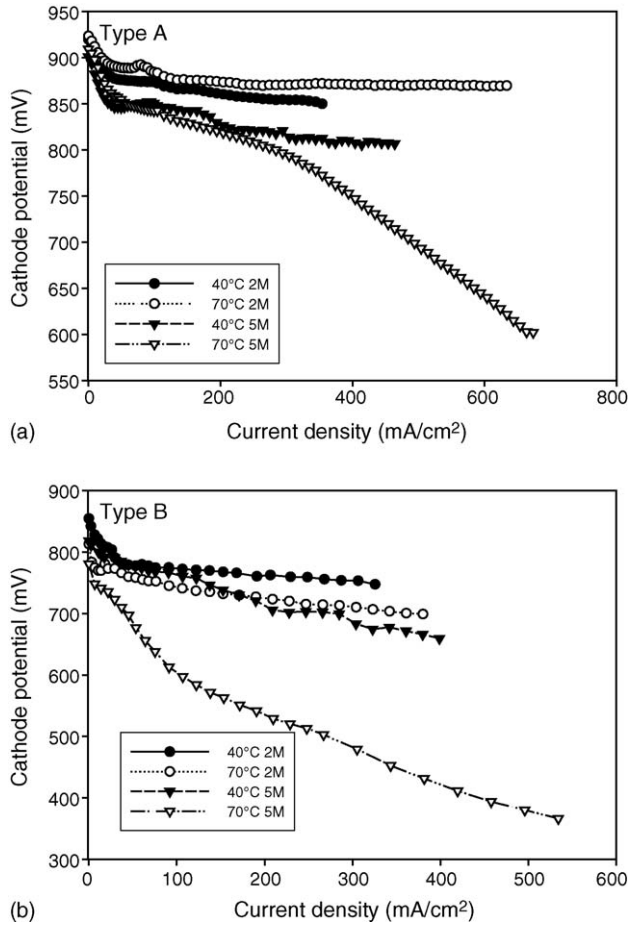

Fig. 3. Comparison of cathode polarization curve (a) type A and (b) type B.

the smaller current value more than the polarization of "type A" MEA. In addition, the former showed worse performances than the latter. Therefore, it can be seen that "type B" showed a higher concentration polarization than "type A" MEA. According to Table 1, the carbon substrates of "type A" MEA and "type B" MEA have different hydrophobicity. This feature affects the removal of water and the mass transfer of methanol and O_2. The removal of water becomes particularly difficult when the electrode is not wet-proofed sufficiently, and water flooding can occur.

As shown in Fig. 3, the cathode polarizations of both types of MEA show similar trends. Unlike the case of the anode, the open circuit potentials of the cathode were affected both by temperature and by the concentration of methanol that was applied into the anode. The effect of methanol concentration on open circuit potentials was more significant for the "type B" MEA using Nafion 115 than for the "type A" MEA using Nafion 117. In addition, at 70 °C above methanol's boiling point, the open circuit potentials decreased sharply for the "type B" MEA. This decrease is due to methanol crossover, which implies a large quantity of methanol crossing the thinner Nafion 115. For both types of MEA, a high temperature, high concentration of methanol and high current caused adrastic polarization loss of the cathode. The cathode polarization of the "type B" MEA was higher in spite of the lower ionic resistance of Nafion 115, which could be due to the larger electro-osmotic drag and methanol permeability of Nafion 115 and the poor mass transfer characteristics of the "type B" MEA' s electrode, as shown in the case of anode polarization.

We did not focus on the optimization of DMFC operation, or on the characterization of electrodes. In order to confirm the generality of our analysis using separated *I–V* curves, we investigated both the "type A" and "type B" MEA that had different efficiencies. The following interpretations with Tafel plots for each electrode are for the "type B" MEA. For the "type A" MEA, the interpretation of results that showed similar trends to the "type B" MEA was also obtained.

Fig. 4 shows Tafel plots for the anode polarization of the "type B" MEA. Each Tafel plot can be divided into several regimes according to the change of slope, as shown in the work on the polarizations of PEMFCs by Jaouen et al. [28]. According to several previous studies on the diagnostics of PEMFCs using Tafel plots, the changes of slope indicate the addition of rate-controlled characteristic resistances [29–31]. For PEMFCs, especially, the doubling of the Tafel slope indicated a shift of the first regime controlled by Tafel kinetics to the second regime controlled by Tafel kinetics and oxygen diffusion or proton migration [28,30]. For DMFCs, it is difficult for Tafel kinetics to adopt the kinetics of methanol oxidation throughout the whole range of the current. Therefore, this theoretical modeling and simulation for PEMFC cannot be directly applied to the case of DMFC. However, it is possible to use this diagnosis to interpret the tendency of polarization under various operating conditions in a DMFC single cell.

The first slopes decreased with an increase of temperature when the same concentration of methanol solution was used, and decreased with an increase of methanol solution concentration at the same temperature. The effect of temperature on the first slopes clearly indicates that there has been an increase in the methanol oxidation reaction rate with an increase of temperature. The concentration of methanol in the feed affects the concentration at the reaction site on the surface of catalyst par-

Table 1
Properties of the electrodes

	Porosity (%)	Thickness (μm)	Wet-proofing	Resistance of carbon substrate (mΩ cm^2)
Type A[a]	78	280	20 wt.% FEP loading	2.2
Type B[b]	76	260	5 wt.% PTFE loading	14

[a] Database from Toray Industry Inc.
[b] Database from SGL carbon group Inc.

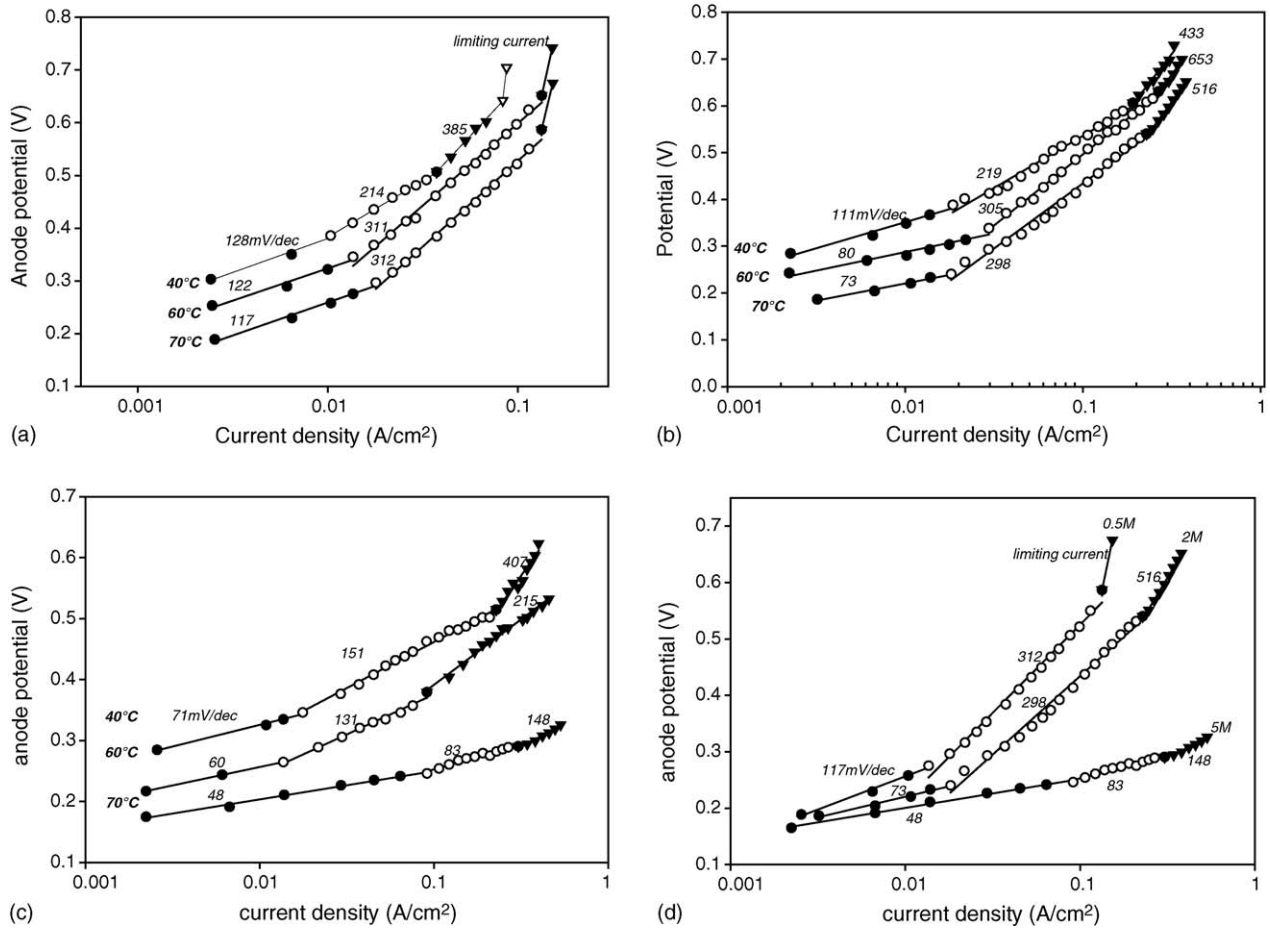

Fig. 4. Tafel plots of anode polarization curve for "type B" MEA: at various temperatures (a) with 0.5 M methanol solution, (b) with 2 M methanol solution, (c) with 5 M methanol solution and (d) with various concentration of methanol at 70 °C.

ticles. The theoretical Tafel slope reflects Tafel kinetics and is independent of the concentration. In this figure, the first regimes of Tafel plots reflect the increased activation of the anode by increasing the temperature, but were affected by the surface concentration at the active region. Therefore, the first slope cannot be interpreted as a theoretical Tafel slope. This indicates that these regimes are somewhat affected by mass transfer and are not determined by Tafel kinetics. For the case of "type A" MEA, which can transport the reactant and product more efficiently than the "type B" MEA, the first slopes of the anode polarizations in the Tafel plots with different methanol concentrations were almost $40 \mp 2\,\mathrm{mV\,dec^{-1}}$. These values are similar to the values found in the studies of Tapan et al. [20]. Therefore, when porous electrodes that can transport reactants more efficiently were used, the regime of the first slope can be interpreted as an activation-controlled regime that is modeled by Tafel kinetics.

The second and third slopes are more complicated. When low concentrations of methanol (0.5 and 2 M) were used, the second (or third) slopes became larger at higher temperatures (60 and 70 °C) and became much larger than twice the first slopes, as expected by Jaouen et al. [28] and Perry et al. [30]. This drastic increase of the slopes implies the introduction of one or more resistances, which generally have a longer characteristic length relative to the rate of the process, such as transport and reaction. In this case, this slope increase could be due to the fact that the supply of methanol by convective flow into the cell is insufficient to compensate for the rapid consumption of methanol on the surfaces of catalyst particles. In other words, the characteristic rate of methanol consumption exceeded the characteristic supply rate of methanol by mass transfer. Especially at higher temperatures, the faster rate of reaction needs a greater amount of methanol. Additionally, the limiting current appeared as the third or fourth slope with 0.5 M methanol solution. On the other hand, when high concentrations of methanol were used, the second slopes decreased with increased temperature. This indicates that the critical resistance due to an insufficient supply of methanol was eliminated and that greater methanol activity, a higher rate of methanol oxidation, a higher diffusion rate of methanol and a higher elimination rate of CO_2 enhanced the cell performance at higher temperatures. Additionally, the second slopes were approximately double the first ones, as shown in the diagnostic studies of PEMFCs. Especially, operations above the methanol boiling point of 64 °C (i.e., at 70 °C) showed much lower polarizations of the anode due to the higher activity of the vaporized methanol. This makes it possible to find an optimal condition for anode performance based on relative reaction rates and mass transfer.

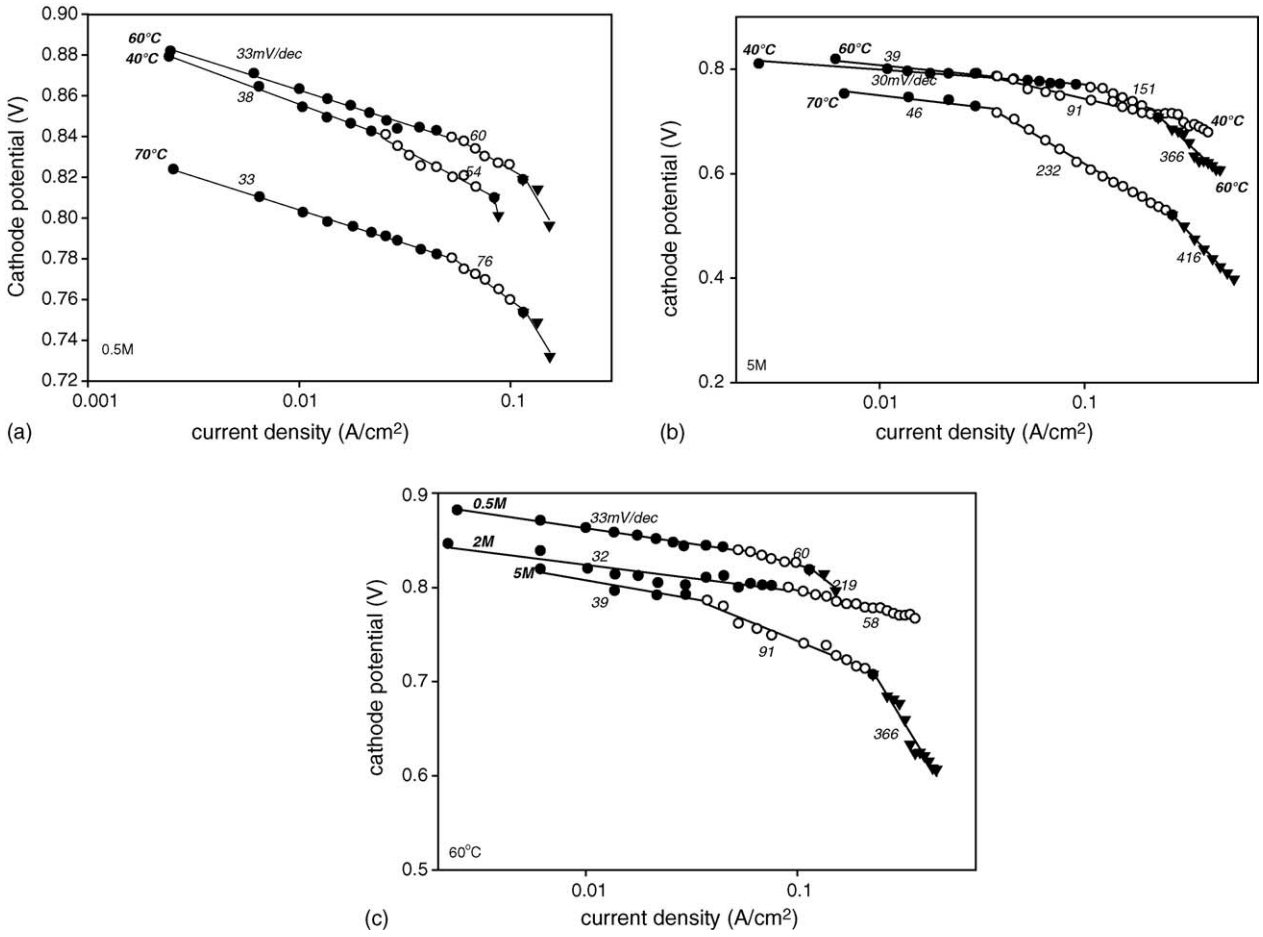

Fig. 5. Tafel plots of cathode polarization curve for "type B" MEA: at various temperatures (a) with 0.5 M methanol solution (b) with 5 M methanol solution and (c) at 60 °C with various concentration of methanol solution.

Fig. 5 shows the Tafel plots for cathode polarization. In Table 2, we have summarized the factors that affect the methanol crossover and mixed potential and their dependence on the operating parameters. According to Ren et al. [15], for Nafion, the diffusion coefficient of methanol increased from 4.15×10^{-6} to 35.7 $cm^2\ s^{-1}$ as the temperature increased from 30 to 130 °C and the activation energy of methanol diffusion was 4.8 kcal mol^{-1}. Methanol concentration in the membrane by absorption increased from 0.040 to 0.391 mol dm^{-3} at 30 °C with an increase of feed concentration from 0.1 to 1.0 mol dm^{-3}. This value was slightly affected by temperatures below the water boiling temperature of 100 °C, and decreased rapidly above this temperature due to the rapid vaporization of the liquid phase. Since methanol permeability is the product of diffusivity and solubility, it increases with increased temperature and concentration. The electro-osmotic drag coefficient increases from 2.2 to 3.0 with an increase of temperature from 40 to 70 °C. At open circuit potentials, only methanol diffusion determines the methanol crossover. As the current density increases, the effect of electro-osmotic drag increases and becomes dominant at ca. 200 mA cm^{-2}, with 1atm of cathode back pressure [32].

Table 2
Summary of the variables that affect methanol crossover

	Temperature ↑	Methanol concentration ↑	Current ↑
Diffusion of methanol	↑	↑	–
Electro-osmotic drag of water and methanol	↑	–	↑
Methanol oxidation rate	↑	↑	↑

Clearly, due to the methanol crossover, the open circuit potentials of were lower than those for the cathodes of a PEMFC, as shown in Fig. 3. The first slopes were approximately the same at 30–40 mV dec^{-1} for almost all cases, except for the cases of high temperature and high methanol concentration, which deviated slightly from this value. In addition, these values are within the ranges of Tafel slopes for PEMFCs predicted by Laurencelle et al. [29]. At this low current density, methanol is transported mainly by diffusion, which is independent of current density. Therefore, this factor is not reflected in the values of the slopes. When the dilute methanol solution was used at low temperatures of 40 and 60 °C, below the methanol boiling point, the second Tafel slopes were approximately the same as or lower than double the first ones. As the current loaded to the cell increased, the amount of methanol transported through the membrane decreased due to the increase of methanol consumption at the anode side [23]. Therefore, the behavior of the Tafel plots

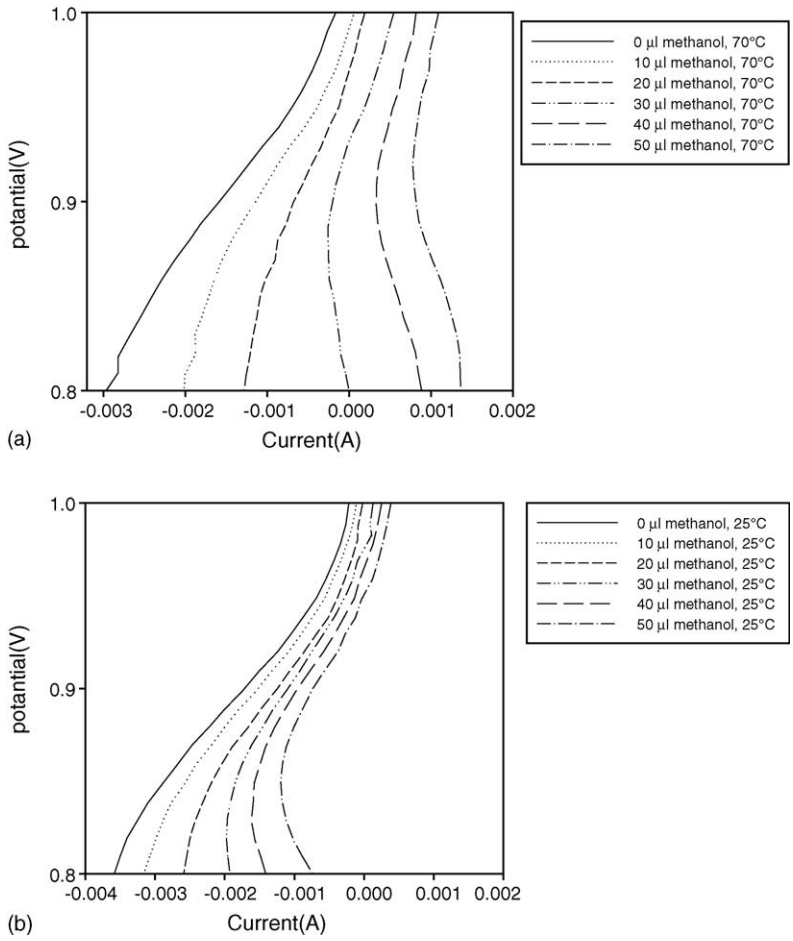

Fig. 6. Oxygen reduction in the presence of methanol (with $HClO_4$ electrolyte solution): (a) at 70 °C and (b) 25 °C.

became similar to that of the plots for PEMFC, even though the overall potential for DMFC's cathode was lower than that for PEMFC's cathode due to its mixed potential.

As the concentration of methanol solution and temperature increased, the slopes, especially the second or third ones, increased sharply. Ren et al. [23] explained that this behavior originated from water flooding due to the electro-osmotic drag flow of water. Indeed, the point at which the slope started to increase sharply is similar to the current at which the electro-osmotic drag started to dominate the transport of water and methanol, as measured by Ren and Gottesfeld [32]. This electro-osmotic drag increases with increasing temperature and current density, which explains the increase of the second slope with increasing temperature and the sharp increase of the third slope at 5 M and 60 °C, respectively. However, the fact that the second and third slopes increase with increased methanol solution concentration cannot be explained simply by water flooding; it could also be due to the electro-osmotic drag of methanol. Usually, the electro-osmotic drag coefficient of methanol can be assumed to be the same as that of water. The transported methanol, the amount of which is linearly proportional to the current density, increased the mixed potential significantly. In addition, the decreased cathode performance became more pronounced as temperatures increased above the methanol boiling point.

Fig. 6 shows the mixed potential of oxygen reduction with methanol oxidation at 20 and 70 °C using the rotating disk electrode. In this figure, the negative current represents the reduction current. As the amount of methanol added into the electrolyte solution increased, the potentials at zero currents and the reductions currents at each potential were decreased, reflecting the mixed potential of oxygen reduction with methanol oxidation. At 70 °C, with the electrolyte containing 40 μl of methanol, the current was entirely shifted to the oxidation current while, at 25 °C, with the same electrolyte composition, the current remained a reduction current throughout the whole region of measurement. This is due to reduced solubility of oxygen into the electrolyte solution and the increased rate of methanol oxidation with the increased temperature.

Fig. 7 shows the effect of the cathode pressure on the open circuit potentials of the cathode. The open circuit potentials of the cathode decreased with the increased pressure due to back diffusion due to the pressure gradient from the anode to the cathode. However, as cell temperature increased, the degree of this enhancement became lower due to the relatively fast diffusion at the higher temperature.

Figs. 8 and 9 show the effect of the methanol flow rate into the anode on electrode polarization using low concentration and high concentration of methanol solution, respectively.

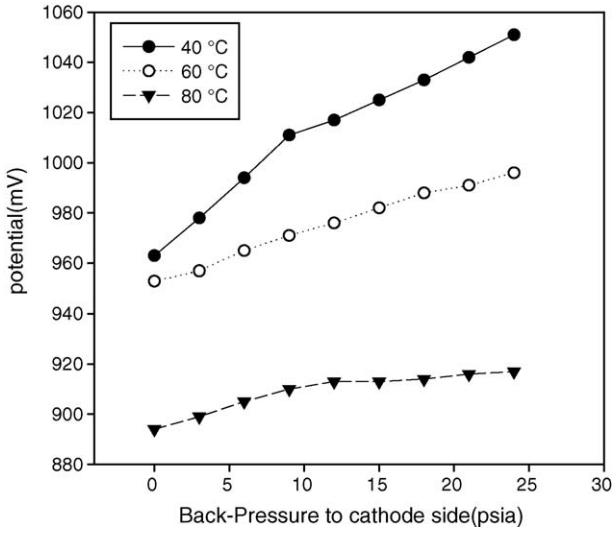

Fig. 7. Effect of cathode pressure on the open circuit potentials of cathode for "type A" MEA.

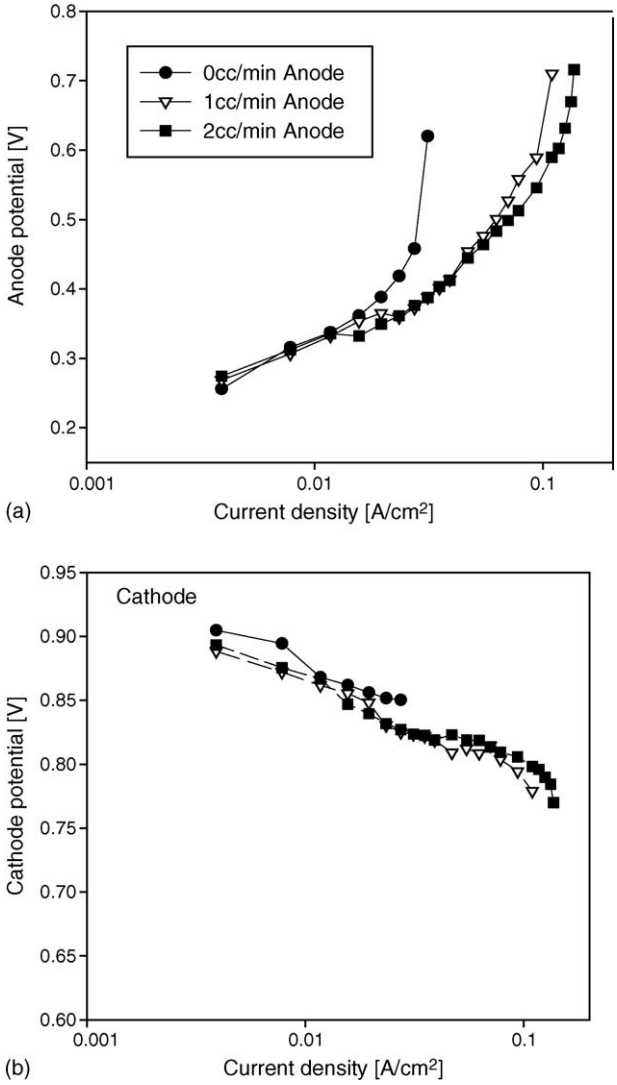

Fig. 8. Effect of methanol flow rate into anode on the performance of anode and cathode with low concentration (0.5 M) of methanol for "type B" MEA: Tafel plots of (a) anode polarization and (b) cathode polarization.

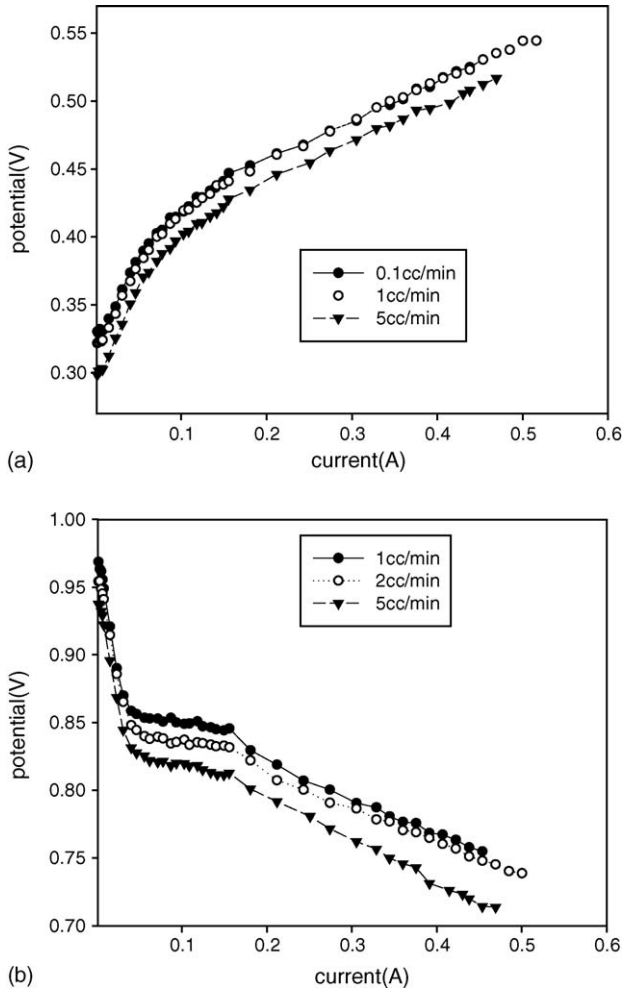

Fig. 9. Effect of methanol flow rate into anode on the performance of anode and cathode with high concentration (2 M) of methanol for "type A": (a) anode polarization curve and (b) cathode polarization curve.

With a low concentration of methanol solution (0.5 M), the effect of the methanol flow rate mainly involved changes in the limiting current for the anode polarization. The increase of limiting current indicates the enhancement of mass transfer by convection. Cathode polarization was not affected by the convection in the anode electrode with the dilute methanol solution.

On the other hand, when a high concentration of methanol solution (2 M) was used, the anode and cathode potential simultaneously decreased with the increase of methanol flow rate. The former is due to the fact that the faster convection increased the concentration of methanol at the anode active site and the latter is due to excess methanol supplied by convection and its crossover through the membrane.

Fig. 10 shows the effect of the O_2 flow rate into the cathode on the electrode polarizations. The O_2 flow rate affected the anode polarization considerably more than the cathode polarization. The anode polarization increased with increased O_2 flow rate, but the increase diminished above 350 cm^3 min^{-1}. This result is consistent with Fig. 11, which represents the effect of cathode pressure on the open circuit potentials of electrodes. According to this figure, the increase of cathode pressure caused an increase

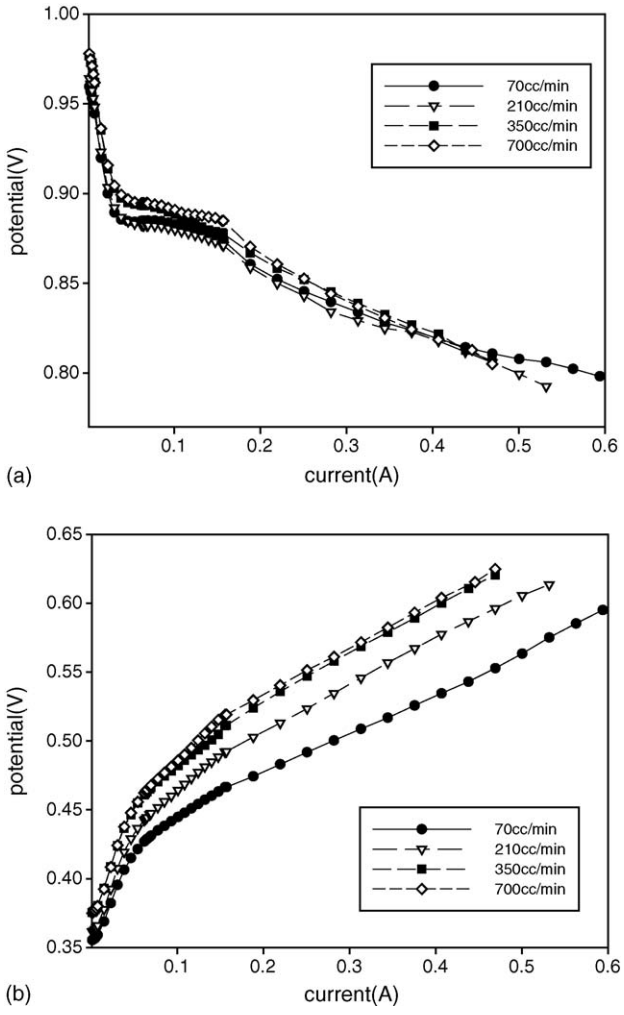

Fig. 10. Effect of O_2 flow rate into cathode on the performance of anode and cathode for "type A" MEA: (a) cathode polarization curve and (b) anode polarization curve.

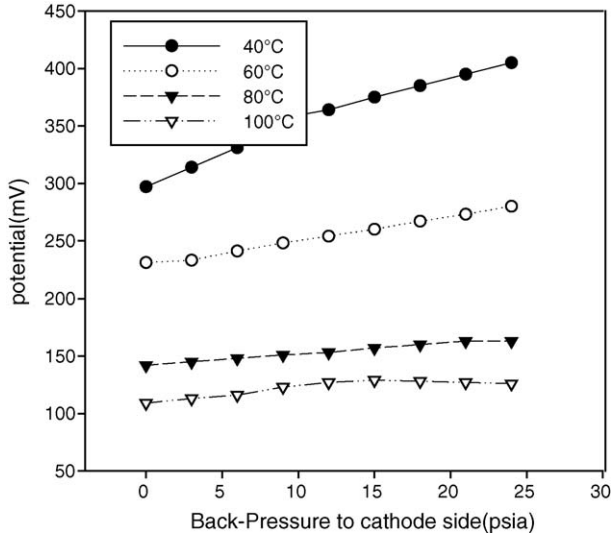

Fig. 11. Effect of cathode pressure on the open circuit potentials of anode and cathode for "type A" MEA.

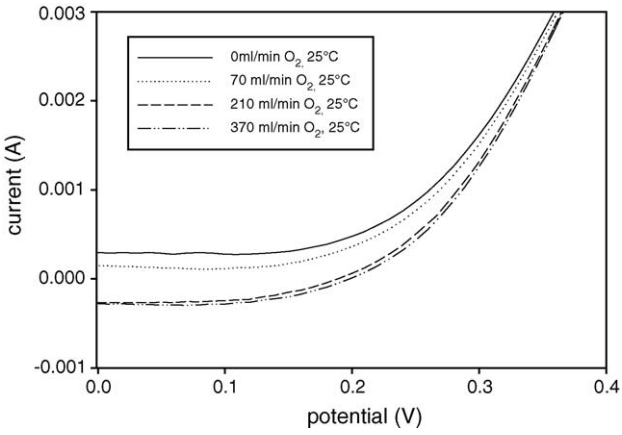

Fig. 12. Methanol oxidation in the presence of oxygen (with $HClO_4$ electrolyte solution).

in the open circuit potential of the anode. The increase of the convection rate of O_2 flow into the cathode (Fig. 10) and the pressure gradient, which increases from the cathode to the anode (Fig. 11), can lead to an increase of O_2 permeation. According to Bernardi and Verbrugge [33], the dissolved O_2 diffusivities are 1.22×10^{-6} cm^2 s^{-1} at 80 °C and 1.69×10^{-6} cm^2 s^{-1} at 95 °C, which are comparable with the methanol diffusivities of 1.6×10^{-5} cm^2 s^{-1} at 90 °C. We also studied the methanol oxidation in the presence of O_2 flow into the electrolyte, using a rotating disk electrode, as shown in Fig. 12. For the methanol oxidation, the presence of O_2 led to an earlier onset of reaction and a lower current density at the each current. Recently, Jusys and Behm [34] studied simultaneous oxygen reduction and methanol oxidation using differential electrochemical mass spectrometry and cyclic voltammetry. They observed not only the mixed potential between the two reactions by simple superimposition, but also the interaction between the two reactions. O_2 can react with methanol and can form incomplete oxidized intermediates such as aldehyde and formic acid, which hinder the completion of methanol oxidation due to their catalyst blocking and competition with methanol. In Fig. 11, the increase of anode potential at zero current with the increase of cathode pressure was slower at higher temperatures. This can result from the fact that the methanol oxidation reaction activates faster and O_2 solubility decreases at higher temperatures.

4. Conclusion

In order to observe the behavior of the anode and the cathode during actual operation of a DMFC and to minimize the polarization of the reference electrode, we used a RHE reference electrode with minimal instability. For the analysis of the *I–V* polarization curve of each electrode, Tafel plots were used as a diagnostic tool. According to the slopes of the Tafel plots, the *I–V* polarization curves of each electrode were divided into the several regimes, which implied an increase of resistance. When the characteristic rate of methanol consumption exceeded the characteristic supply rate of methanol by mass transfer, the anode polarization increased sharply. In addition, the effects of operating parameters such as the concentration of methanol,

temperature, and the flow rates of reactants on the performance of each electrode, were interpreted in terms of mass transfer and electrode activation. The methanol and oxygen crossover through the electrolyte membrane affected the performance of cells significantly and these crossovers were studied with various experimental systems.

Acknowledgement

This research was funded by the Brain Korea 21 (BK 21). This research was partially funded by Center for Ultramicrochemical Process Systems (2004–2005) sponsored by KOSEF.

References

[1] K. Scott, W.M. Tamma, P. Argyropoulos, J. Power Sources 79 (1999) 43–59.
[2] Z. Qi, A. Kaufman, J. Power sources 110 (2002) 177–185.
[3] M.W. Verdrugge, J. Electrochem. Soc. 136 (1989) 417–423.
[4] P.S. Kauranen, E. Skou, J. Appl. Electrochem. 26 (1996) 909–917.
[5] J. Cruickshank, K. Scott, J. Power Sources 70 (1998) 40–47.
[6] V.M. Barragán, C. Ruiz-Bauzá, J.P.G. Villaluenga, B. Seoane, J. Power Sources 130 (2004) 22–29.
[7] X. Ren, W. Henderson, S. Gottesfeld, J. Electrochem. Soc. 144 (1997) L267–L270.
[8] S.R. Narayanan, A. Kinder, B. Jeffries-Nakamura, W. Chun, H. Frank, M. Smart, T.I. Valdez, S. Surampudi, G. Halpert, J. Kosek, C. Cropley, Annu. Battery Conf. Appl. Adv. 11 (1996) 113–122.
[9] V. Gogel, T. Frey, Z. Yongsheng I, K.A. Friedrich, L. Jörissen, J. Garche, J. Power Sources 127 (2004) 172–180.
[10] B.S. Pivovar, M. Hickner, T.A. Zawodzinski Jr., X. Ren, S. Gottesfeld, in: S.R. Narayanan, S. Gottesfeld, T. Zawodzinski (Eds.), Direct Methanol Fuel Cells, The Electrochemical Society Proceedings Series, Pennington, NJ, 2000, pp. 221–225.
[11] T.I. Valdez, S.R. Narayanan, in: S. Gottesfeld, T.F. Fuller (Eds.), Proton Conducting Membrane Fuel Cells II, The Electrochemical Society Proceedings Series, Pennington, NJ, 1998, pp. 380–381.
[12] J.A. Drake, W. Wilson, K. Killeena, J. Electrochem. Soc. 151 (2004) A413–A417.
[13] H. Dohle, J. Divisek, J. Mergel, H.F. Oetjen, C. Zingler, D. Stolten, J. Power Sources 105 (2002) 274–282.
[14] V. Gogel, T. Frey, Z. Yongsheng I, K.A. Friedrich, L. Jörissen, J. Garche, J. Power Sources 127 (2004) 172–180.
[15] X. Ren, T.E. Springer, T.A. Zawodzinski, S. Gottesfeld, J. Electrochem. Soc. 147 (2000) 464–474.
[16] Z. Qi, A. Kaufman, J. Power Sources 110 (2002) 177–185.
[17] A. Heinzel, V.M. Barragán, J. Power Sources 84 (1999) 70–74.
[18] B. Gurau, E.S. Smotkin, J. Power Sources 112 (2002) 339–352.
[19] C. Lim, C.Y. Wang, J. Power Sources 113 (2003) 145–150.
[20] N.A. Tapan, W.E. Mustain, G. Gurau, G. Sandi, J. Prakash, J. N. Mater. Electrochem. Syst. 7 (2004) 281–286.
[21] J.C. Amphlett, B.A. Peppley, E. Halliop, A. Sadiq, J. Power Sources 96 (2001) 204–213.
[22] H. Dohle, K. Wippermann, J. Power Sources 135 (2004) 152–164.
[23] X. Ren, T.E. Springer, S. Gottesfeld, J. Electrochem. Soc. 147 (2000) 92–98.
[24] A. Kuver, I. Vogel, W. Vielstich, J. Power Sources 52 (1994) 77–80.
[25] A. Kuver, W. Vielstich, J. Power Sources 74 (1998) 211–218.
[26] S. Mitsushima, N. Araki, N. Kamiya, K. Ota, J. Electrochem. Soc. 149 (2002) A1370–A1375.
[27] B. Gurau, R. Viswanathan, R. Liu, T.J. Lafrenz, K.L. Ley, E.S. Smotkin, E. Reddington, A. Sapienza, B.C. Chan, T.E. Mallouk, S. Sarangapani, J. Phys. Chem. B 102 (1998) 9997–10003.
[28] F. Jaouen, G. Lindberg, G. Sundholm, J. Electrochem. Soc. 149 (2002) A437–A447.
[29] F. Laurencelle1, R. Chahine, J. Hamelin, K. Agbossou, M. Fournier, T.K. Bose, A. Laperriere, Fuel Cells 1 (2001) 66–71.
[30] M.L. Perry, J. Newman, E.J. Cairns, J. Electrochem. Soc. 145 (1998) 5–15.
[31] L. Pisani, M. Valentini, G. Murgia, J. Electrochem. Soc. 150 (2003) A1549–A1559.
[32] X. Ren, Gottesfeld, J. Electrochem. Soc. 148 (2001) A87–A93.
[33] D.M. Bernardi, M.W. Verbrugge, J. Electrochem. Soc. 139 (1992) 2477–2490.
[34] Z. Jusys, R.J. Behm, Electrochim. Acta 49 (2004) 3891–3900.